PROCEEDINGS OF
INTERNATIONAL CONFERENCE ON NEW TRENDS IN APPLIED SCIENCES
https://proceedings.icontas.org/
International Conference on New Trends in Applied Sciences (ICONTAS'23), Konya, December 1-3, 2023.

A RECOGNITION METHOD OF R-PEAKS ON ELECTROCARDIOGRAMS BASED ON WAVELET TRANSFORM WITH PSEUDO-DIFFERENTIAL OPERATORS

Yuta YOSHIKAWA, Takayuki OKAI, Hidetoshi OYA
Tokyo City University,
0009-0001-6576-527X, 0009-0002-5358-8429, 0000-0003-1046-5832
g2281462@tcu.ac.jp, okai@cae-sc.com, hide@tcu.ac.jp

Minoru YOSHIDA, Md.Masudur RAHMAN
Kanagawa University
0000-0001-5316-5958, 0009-0008-6927-7418
washizuminoru@hotmail.com, Masudur_2006@yahoo.com

ABSTRACT: In this paper, we propose a recognition method of R-peaks on electrocardiograms (ECGs) based on wavelet transform with pseudo-differential operators. It is well known that the accurate recognition of R-peaks is highly importance for diagnosis of cardiac diseases and autonomic ataxia. However, the existing results for detection of R-peaks are not always accurate and can have missed peaks or false. Difficulties in accurate R-peaks detection is caused by presence of various noises in ECGs and the physiological variability of the QRS complex. From the above, we propose a more flexible and adaptive recognition method of R-peaks. In order to develop the proposed detection method, noises, artifacts, and baseline variation in ECGs are firstly suppressed by using the low-pass/high-pass filters, moving average, and MaMeMi filter. Next, the time-frequency domain's energy distribution is computed by using wavelet transform with pseudo-differential operators. Furthermore, we introduce a time-series index, f^p-Normalized Spectrum Index (f^p-*NSI*) obtained by scalograms based on the wavelet transform with pseudo-differential operators. Finally, R-peaks are recognized by taking the threshold toward the results of f^p-*NSI*. In this paper, we present the proposed recognition method of R-peaks on ECGs, and the effectiveness (accuracy) of the proposed method is evaluated.

Key words: R-peaks, Wavelet transform, Pseudo-differential operators, Electrocardiograms, MaMeMi filter

INTRODUCTION

ElectroCardioGrams (ECGs) reflect the electrical activity of the myocardium, and cardiac conditions can be detected. Therefore, it is known to be useful for diagnosing cardiac diseases such as arrhythmias. For example, discriminating each state of ECG waveforms (Okai, T. et al., 2021) and predicting the effectiveness of electrical defibrillation (Yoshikawa, Y. et al., 2022) have been proposed, and these problems are very important for raising life-saving rates. Furthermore, the problem of detecting R-peaks is also essential; specifically, the R-R interval affects the autonomic nervous of a tense state. Therefore, accurate detection of R-peak would be helpful for a diagnosis of autonomic ataxia.

In this way, some methods have been proposed for detecting R-peaks such as wavelet transform (Merah, M. et al., 2015), moving average and Hilbert transform (Manikandan, M. S., & Soman, K. P., 2012), non-linear filter (Kohler. B. U. et al., 2002), and so on. One approach is to denoise and suppress the cardiac baseline by using a MaMeMi filter (Castells-Rufas, D. et al., 2015) and this method can detect the normal peak, however, the detection rate was decreased when abnormal conditions were occurring. Therefore, we considered that a more flexible and adaptive R-peaks detection method is required.

In this paper, we propose the R-peaks detection algorithm based on wavelet transform with pseudo-differential operators. In order to construct the proposed algorithm, various noises, artifacts, and baseline variation in ECGs are firstly suppressed by using the low-pass/high-pass filters, moving average, and MaMeMi filter. Next, the time-frequency domain's energy distribution is calculated by using wavelet transform with pseudo-differential operators. In particular, by changing some functions in pseudo-differential operators, the energy's prominence can be adjusted. Furthermore, from the result of wavelet transform with pseudo-

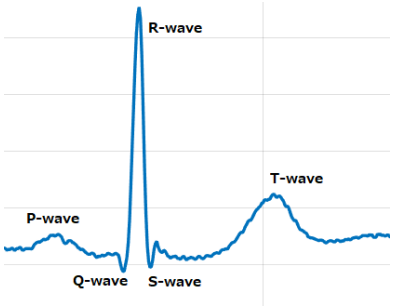

Figure 1. The Composition of Normal Sinus Rhythm (SR)

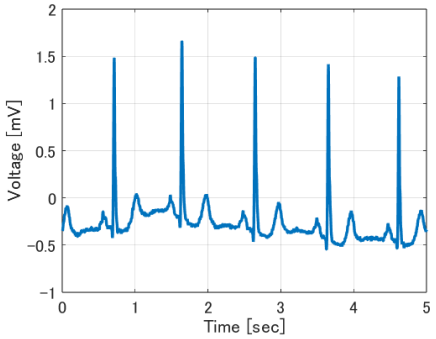

Figure 2. The Example of Sinus Rhythm (SR)

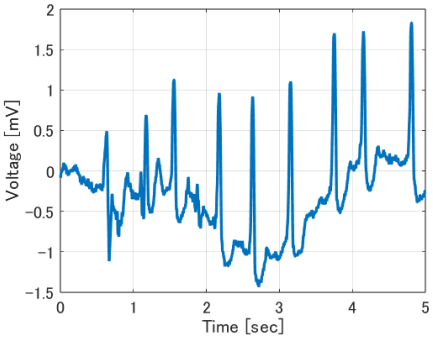

Figure 3. Abnormal Condition of ECGs

differential operators, we introduce a time series index: f^p-Normalized Spectrum Index (f^p-*NSI*) is computed. This measure can capture energy transition in time variation, and characteristics of the peak portion can be

ELECTROCARDIOGRAMS

ECG waveforms

The normal rhythmic state of the heart is defined as normal Sinus Rhythm (SR). The SR consists of P-wave, QRS complex-waves, and T-wave, and the composition of SR is shown in Figure 1. In normal SR, this kind of ECG (i.e., P-wave, QRS complex-waves, and T-wave) appears 60-80 times per minute, and an example of the SR waveform is shown in Figure 2. Moreover, detecting R-peak in abnormal cardiac conditions is also essential for providing medical care according to the respective state, and accurate detection is necessary in these conditions. Here, the abnormal state of ECG is shown in Figure 3.

Database

The database of this study utilizes MIT-BIH, and this data set is accumulating for analysis of arrhythmias by the Massachusetts Institute of Technology. Furthermore, the sampling rate is 360 [Hz] and labeled by two or more cardiologists (Moody, G. B. et al., 2001). Note that in this study, the ECG waveforms are cut out for 5 [sec] and applied with 50% overlap to the next subject of analysis.

PROPOSED DETECTION METHOD

Preprocessing

In this paper, we adopt a low-pass/high-pass filter, moving average, and MaMeMi filter in preprocessing phase. First of all, we introduce the low-pass/high-pass filter into the original signal: $x(t)$, and various noises (e.g. heart rate variability, other artifacts, and so on) are suppressed. Note that, the low-pass filter with Kaizer-window and the elliptic high-pass filter are utilized, and these filters are designed by MATLAB algorithm. Furthermore, the cut-off frequency is set at 20 [Hz] of the low-pass filter and 1 [Hz] for the high-pass filter, respectively. Here, the original signal: $x(t)$ and filtered signal: $x^*(t)$ are shown in Figure 4, 5. Next, we utilize

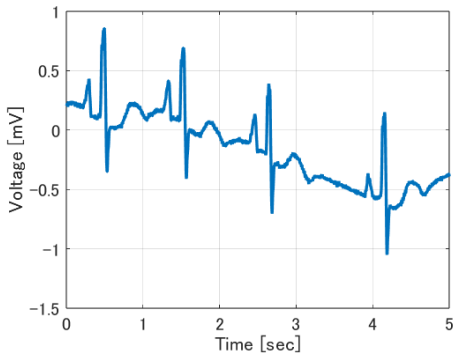

Figure 4. Original Signal $\boldsymbol{x(t)}$

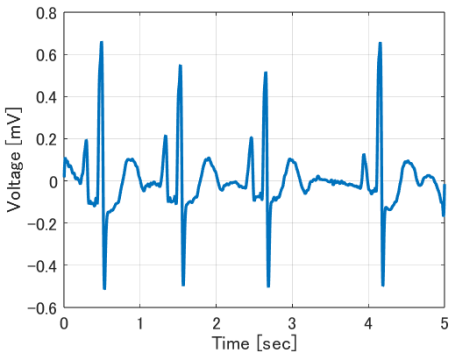

Figure 5. Low-pass / High-pass Filtered Output $\boldsymbol{x^*(t)}$

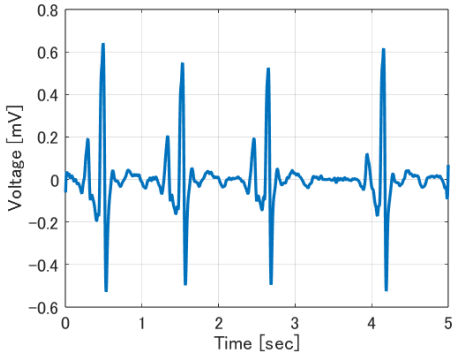

Figure 6. Moving Averaged Signal $\boldsymbol{m(t)}$

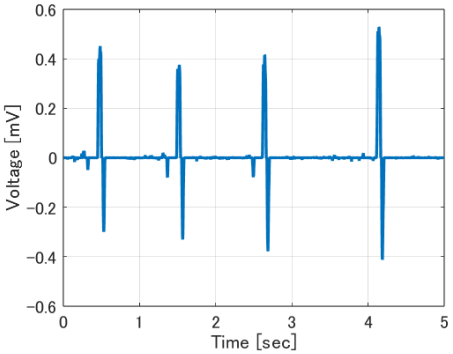

Figure 7. MaMeMi Filtere and Output $\boldsymbol{h(t)}$

to the moving average to suppress the baseline variation, and the window size is set as 72 [samples]. The moving averaged signal: $\boldsymbol{m(t)}$ is shown in Figure 6. Moreover, MaMeMi filter (Castells-Rufas, D. et al., 2015) is used, and can remove the ingredient of the signal that is not relevant for peak. The output $\boldsymbol{h(t)}$ of MaMeMi filter can be derived as

$$\boldsymbol{h(t) = m(t) - \frac{max^*(t) + min^*(t)}{2}}$$

$$\boldsymbol{max^*(t) = \begin{cases} m(t) & if\ t = 0 \\ max^*(t-1) + \sigma \cdot \Delta & if\ m(t) > max^*(t-1) \\ max^*(t-1) - \Delta & if\ m(t) \leq max^*(t-1) \end{cases}}$$

$$\boldsymbol{min^*(t) = \begin{cases} m(t) & if\ t = 0 \\ min^*(t-1) - \sigma \cdot \Delta & if\ m(t) < min^*(t-1) \\ min^*(t-1) + \Delta & if\ m(t) \geq min^*(t-1) \end{cases}}$$

Here, $\boldsymbol{\sigma}$ and Δ are parameters, and the best parameters are reported $\boldsymbol{\sigma = 2.0}$ and $\boldsymbol{\Delta = 2.0}$, respectively (Castells-Rufas, D. et al., 2015). However, these parameters are insufficient to capture the characteristics of peaks. Therefore, in this paper, these parameters are selected experimentally and set to $\boldsymbol{\sigma = 4.0}$ and $\boldsymbol{\Delta = 5.0 \times 10^{-3}}$, respectively. The output $\boldsymbol{h(t)}$ of MaMeMi filter is shown in Figure 7.

Wavelet transform with pseudo-differential operators

In this section, the wavelet transform with pseudo-differential operators is presented. First of all, we show the wavelet transform, which is one of the time-frequency analysis methods and captures the frequency components in time variation. The continuous wavelet transform is defined as

$$\boldsymbol{W_\psi(a,b) \triangleq \frac{1}{\sqrt{|a|}} \int_{-\infty}^{+\infty} f(t) \overline{\psi\left(\frac{t-b}{a}\right)}\, dt,} \quad (1)$$

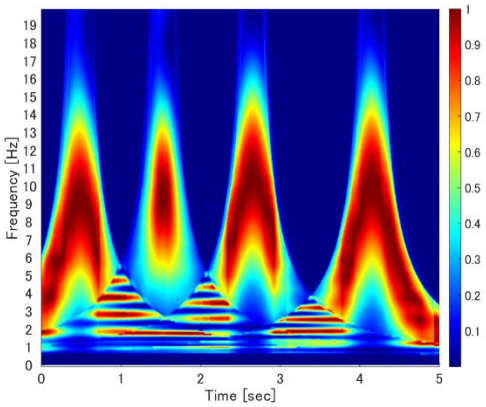

Figure 8. $\boldsymbol{E(a,b)}$ for Figure 7

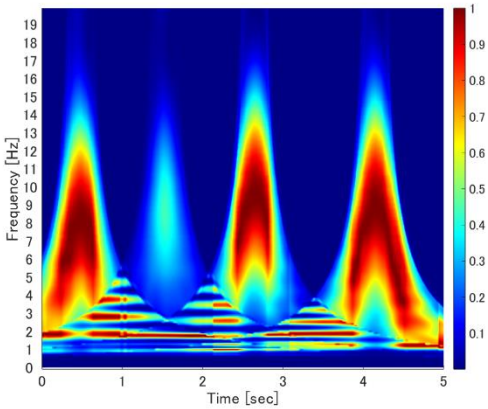

Figure 9. $\boldsymbol{E_{pdo}(a,b)}$ for Figure 7

where, $\boldsymbol{a}$ denotes the scale parameter, $\boldsymbol{b}$ denotes the shift parameter, and the mother wavelet $\boldsymbol{\psi(t)}$ is set as a Gabor wavelet, minimizing the uncertainty principle. Furthermore, we compute the energy distribution from the result of the wavelet transform, and it's called scalogram. Scalogram $\boldsymbol{E(a,b)}$ is calculated as

$$\boldsymbol{E(a,b) = \left|W_{\psi}(a,b)\right|^{2}}, \tag{2}$$

and an example of $\boldsymbol{E(a,b)}$ is shown in Figure 8. Here, we introduce the pseudo-differential operators. Note that, the pseudo-differential operators of the Fourier transform is defined as

$$\boldsymbol{(Ff')(t) \triangleq -j\omega\hat{f}(\omega)} \tag{3}$$

where, $\boldsymbol{F}$ means the Fourier transform, $\boldsymbol{f'(t)}$ denotes $\frac{d}{dt}\boldsymbol{f(t)}$, and $\boldsymbol{\hat{f}(\omega)}$ is the Fourier transform of $\boldsymbol{f(t)}$. Next, it extends this operation to wavelet transform, and it's defined as wavelet transform with pseudo-differential operators. Wavelet transform with pseudo-differential operators is computed from two measurable functions $\boldsymbol{L}$ and $\boldsymbol{H}$, and $\boldsymbol{L}$ means the pseudo-differential operators and H denotes the non-linear function, respectively, and these functions adjust to the emphasis portion of scalogram (Rahman, M. M. et. al, 2022). In this way, the wavelet transform with pseudo-differential operators $\boldsymbol{E_{pdo}(a,b)}$ and is defined as

$$\boldsymbol{E_{pdo}(a,b) \triangleq H\{L(a) \cdot W_{\psi}(a,b)\}}. \tag{4}$$

In this paper, we select the $\boldsymbol{L(a) = a^{\frac{1}{4}}}$ and $\boldsymbol{H(y) = |y|^{2.3}}$, respectively, and these functions are experimentally determined. Here, the example of $\boldsymbol{E_{pdo}(a,b)}$ is shown in Figure 9. In comparison with $\boldsymbol{E(a,b)}$ in Figure 8, one can see that the energy width is narrowed.

$\boldsymbol{f^p}$-Normalized Spectrum Index ($\boldsymbol{f^p}$-*NSI*)

In this section, we introduced the $\boldsymbol{f^p}$-Normalized Spectrum Index ($\boldsymbol{f^p}$-*NSI*) based on ***NSI*** (Okai, T., et al., 2018). $\boldsymbol{f^p}$-*NSI* is a time series signal composed of the centroid frequency of $\boldsymbol{E_{pdo}(a,b)}$, which is calculated as follows

$$\boldsymbol{f^p\text{-}NSI(b) = \frac{\sum_{a=1}^{N} E_{pdo}(a,b) f_r^p(a)}{\sum_{a=1}^{N} E_{pdo}(a,b)}}. \tag{5}$$

Where, p denotes the weighting parameter for frequency component and it is set at $p = 3$ in this paper. Furthermore, we adopt the smoothing method for the result of f^p-*NSI* by using the moving average, and the window size is 30 [samples] and show an example of f^p-*NSI* in Figure 10.

Detection Algorithm

The following procedure is the proposed R-peak detection algorithm:

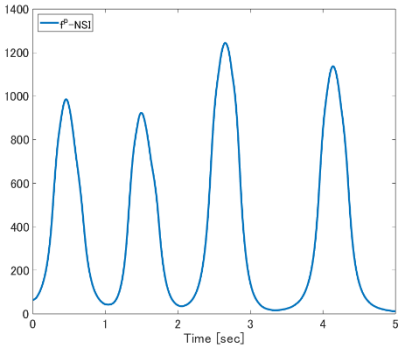

Figure 10. f^p-NSI from $E_{pdo}(a, b)$ for Figure 9

1. Execute preprocessing by using low-pass/high-pass filter, moving average, and MaMeMi filter for target ECG signal.
2. Next, f^p-NSI is calculated from wavelet transform with pseudo-differential operators.
3. Detect the peak position of f^p-NSI that satisfies the following conditions:
   - f^p-NSI width ≥ 36 [samples]
   - f^p-NSI magnitude ≥ 150
4. The detected peak ± 36 [samples] ($\pm$ 0.1 [sec]) is defined as R-peak.

RESULTS AND DISCUSSION

Evaluation Indices

In order to evaluate the proposed recognition method, Recall (R_c), Precision (P_s), Error-ratio (E_r), Accuracy (A_c), and F-measure (F) are adopted, and these indices are computed from TP, FP, and FN. TP means the number of correct detections of R-peaks, FP is the number of actual peaks but not detected, and FN denotes the number of judge peaks but not actual peaks. The indices R_c, P_s, E_r, A_c, and F are computed as follows,

$$R_c = \frac{TP}{TP + FN},$$

$$P_s = \frac{TP}{TP + FP},$$

$$E_r = \frac{FP + FN}{TP},$$

$$A_c = \frac{TP}{TP + FN + FP},$$

$$F = \frac{2 \times P_s \times R_c}{P_s + R_c}$$

Results

First of all, the evaluation results are shown in Table. 1. From the result of Table. 1, the results R_c: 99.58 %, P_s: 99.68 %, and E_r: 0.75 % are obtained. These results surpassed the existing value of R_c : 99.43 %, P_s: 99.67 %, and E_r: 0.88 % (Castells-Rufas, D. et al., 2015). Furthermore, records No. 203 and 207 in MIT-BIH are the most errors occurred in the existing one (i.e., a total of 402 errors). However, the proposed detection algorithm only has 308 errors in the total of records No. 203 and 207, the improvement of detection accuracy for difficult

Table 1. Evaluation Results

R_c	P_s	E_r	A_c	F
99.58 %	99.68 %	0.75 %	99.26 %	99.63 %

records has been well achieved. Consequently, the proposed recognition method is more desirable for result for detection of R-peaks

CONCLUSION

In this paper, the new R-peaks detection algorithm by using the wavelet transform with pseudo-differential operators has been proposed. In order to construct the proposed algorithm, noises, artifacts, and baseline variation in ECGs are firstly suppressed by using the low-pass/high-pass filters, moving average and MaMeMi filter. Next, the time-frequency domain's energy distribution is obtained by using wavelet transform with pseudo-differential operators. Furthermore, from the result of wavelet transform with pseudo-differential operators, a time series index f^p-Normalized Spectrum Index (f^p-NSI) is calculated. Finally, R-peaks are detected by taking the threshold toward the results of f^p-NSI. As a result, the proposed method can achieve 99.58 % of R_c, 99.68 % of P_s, and 0.75 % of E_r, and this result is exceeded in the existing method (Castells-Rufas, D. et al., 2015). i.e. the proposed algorithm is effective for R-peaks detection.

For future work, we will consider the more effective preprocessing and feature detection methods (i.e. more appropriate functions for pseudo-differential operators). So as to improve the detection accuracy for the R-peaks.

ACKNOWLEDGMENT

This research was supported by Grant-in-Aid for Scientific Research (C) No. 20K04555 from Japan Society for Promotion of Science (JSPS).

REFERENCES

Castells-Rufas, D., & Carrabina, J. (2015). Simple real-time QRS detector with the MaMeMi filter. *Biomedical Signal Processing and Control*, 21, 137-145.

Kohler. B. U., Henning, C., & Orglmeister, R. (2002). The Principles of software QRS detection. *IEEE Engineering in Medicine and Biology Magazine*, 21(1), 42-57.

Manikandan, M. S., & Soman, K. P. (2012). A novel method for detecting R-peaks in electrocardiogram (ECG) signal. *Biomedical Signal Processing and Control*, 7(2), 118-128.

Merah, M., Abdelmalik, T. A., & Larbi, B. H. (2015). R-peaks detection based on stationary wavelet transform. *Computer Methods and Programs in Biomedicine*, 121(3), 149-160.

Moody, G. B., & Mark, R. G. (2001). The impact of the MIT-BIH arrhythmia database. *IEEE Engineering in Medicine and Biology Magazine*, 20(3), 45-50.

Okai, T., Akimoto, S., Oya, H., Nakano, K., Miyauchi, H., & Hoshi, Y. (2021). A new recognition system based on gabor wavelet transform for shockable electrocardiograms. *Journal of Applied Life Science International*, 23(12), 40-51.

Okai, T., Hirata, S., Oya, H., Hoshi, Y., & Nakano, K. (2018). A new recognition algorithm for shockable arrhythmias and its performance analysis. *Proc. of 44th Annual Conference of the IEEE Industrial Electronics Society*, 2671-2676.

Rahman, M. M., Kagawa, T., Kawasaki, S., Nagai, S., Okai, T., Oya, H., Yahagi, Y., & Yoshida M. W. (2022). Various scalographic representation of electrocardiograms through wavelet transform with pseudo-differential operators like operators. *Journal of Advanced Simulation in Science and Engineering*, 9(1), 96-112.

Yoshikawa, Y., Okai, T., Oya, H., Hoshi, Y. & Nakano, K. (2022). A prediction system for the effect of electrical defibrillation based on efficient combinations for feature parameters. *Proc. of International Conference on Control, Automation and Information Science (ICCAIS)*, 48-53.